Strategies for protein-based nanofabrication: Ni^{2+}-NTA as a chemical mask to control biologically imposed symmetry

Michael J Dabrowski[1], Jing Ping Chen[1], Huaiqiu Shi[2], Wei-Chun Chin[2] and William M Atkins[1]

Background: Technologies that improve control of protein orientation on surfaces or in solution, through designed molecular recognition, will expand the range of proteins that are useful for biosensors, molecular devices and biomaterials. A limitation of some proteins is their biologically imposed symmetry, which results in indistinguishable recognition surfaces. Here, we have explored methods for modifying the symmetry of an oligomeric protein that exhibits useful self-assembly properties.

Results: *Escherichia coli* glutamine synthetase (GS) contains 24 solvent-exposed histidines on two symmetry-related surfaces. These histidines drive a metal-dependent self-assembly of GS tubes. Immobilization of GS on the affinity resin Ni^{2+}-NTA followed by on-column modification with diethyl pyrocarbonate affords asymmetrically modified GS that self-assembles only to the extent of 'short' dimeric GS tubes, as demonstrated by electron microscopy, dynamic light scattering and atomic force microscopy. The utility of Ni^{2+}-NTA as a chemical mask was also demonstrated for asymmetric modification of engineered cysteines adjacent to the natural histidines.

Conclusions: Current genetic methods do not provide distinguishable recognition elements on symmetry-related surfaces of biologically assembled proteins. Ni^{2+}-NTA serves as a mask to control chemical modification *in vitro* of residues within symmetry-related pairs, on proteins containing functional His-tags. This strategy may be extended to modification of a wide range of amino acids with a myriad of reagents.

Addresses: [1]Department of Medicinal Chemistry, Box 357610, and [2]Center for Bioengineering, Box 351720, University of Washington, Seattle, WA 98195-7610.

Correspondence: William M Atkins
E-mail: winky@u.washington.edu

Key words: atomic force microscopy, histidine tag proteins, molecular self-assembly, protein engineering, proteins on surfaces

Received: **17 August 1998**
Revisions requested: **7 September 1998**
Revisions received: **7 October 1998**
Accepted: **8 October 1998**

Published: **13 November 1998**

Chemistry & Biology December 1998, **5**:689–697
http://biomednet.com/elecref/1074552100500689

Introduction

Although the commercial utility of protein-based devices remains speculative, proposed applications include biosensors, bio-optics, drug delivery and other biomaterials [1–4]. Ultimately, the range of applications might be limited only by our ability to design proteins with novel properties. Design of novel protein-based materials requires controlled deposition of proteins on surfaces or specific arrangement of the individual components in multiprotein aggregates [5–7]. Recombinant DNA methods are used routinely to achieve such control. Fusion-protein technologies that exploit specific binding domains of glutathione S transferase, streptavidin or maltose-binding protein exemplify the strategy of incorporating 'molecular handles' into proteins for attachment to their cognate receptors on functionalized surfaces [8,9]. Similar approaches include incorporation of 'histidine tags' and surface cysteines. Through incorporation of cysteines or histidines at strategic locations, the specific orientation of many proteins at gold surfaces or metal-chelating lipid interfaces can be controlled [10–14]. Although these strategies are adaptable to many proteins, their utility may be severely limited for more complex, multisubunit proteins that possess high-order symmetry, or proteins for which amino-acid substitutions leads to unanticipated changes in expression, stability or function. For complex oligomeric proteins, their inherent symmetry might prevent fabrication of self-assembled aggregates with distinguishable molecular surfaces. For example, tetrameric streptavidin is a commonly used biotechnology reagent exploited for affinity technologies and as a 'molecular adapter' for construction of complex multicomponent arrays of defined molecular topology [15,16]. Due to the symmetry of the streptavidin tetramer, however, any changes within the protein architecture introduced by recombinant DNA methods will be expressed on all equivalent surfaces within the tetramer. An elegant method for bypassing the biologically imposed symmetry involved denaturation and refolding, *in vitro*, of mixtures containing chemically distinguishable streptavidin variants. Upon refolding, it was possible to isolate streptavidin chimeras with chemically distinguishable molecular surfaces that might be useful in drug-delivery protocols or nanofabrication [16].

This approach, however, requires the ability to reversibly denature the biologically assembled aggregate and to isolate the resulting chimeras. In as much as many

Figure 1

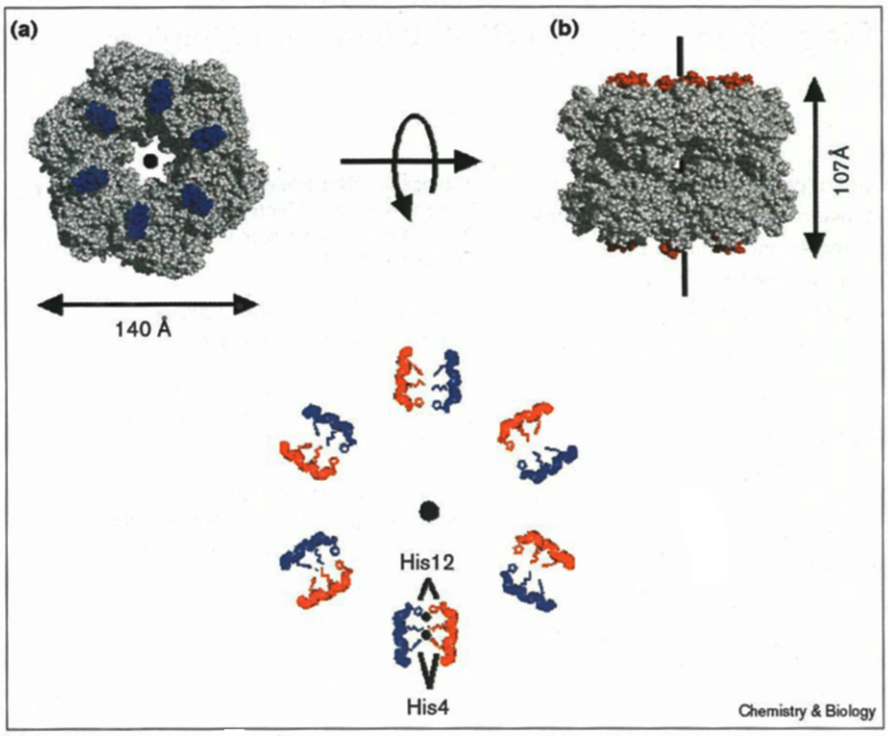

Dodecameric ring structure of glutamine synthetase (GS). **(a)** Face-on view along the six-fold axis of symmetry (black dot) that runs through the ring structure. The amino-terminal helix of each subunit is shown (blue). The outer diameter of the ring structure is 140 Å. **(b)** Edge-on view with the six-fold axis rotated to run vertically. The amino-terminal helix on each subunit is shown now in red. The vertical height of the dodecamer is 107 Å. **(c)** Two GS dodecamers have been stacked along the six-fold axis, which is oriented as in (a), and all residues other than the set of amino-terminal helices at the protein–protein interface have been removed. One GS dodecamer provides the blue helices and the second provides the red helices. At each helix–helix interface, two metal-binding sites are generated, between His4s and His12s. The sidechain of Met8 is also shown. Moving from the sixfold axis of symmetry towards the outer diameter of the ring structure, each helix–helix pair presents two His12s, two Met8s and two His4s.

oligomeric proteins can not be refolded with high yield to homogeneous ensembles, strategies that allow for introduction of asymmetry in complex protein aggregates might expand the range of proteins that can be exploited as 'scaffolds' or 'adapters' in protein-based materials. Here, we demonstrate with glutamine synthetase (GS) the utility of a commonly used affinity resin, Ni^{2+}-NTA, as a chemical mask that allows for controlled, asymmetric, chemical modification of proteins with useful self-assembly properties.

Escherichia coli GS is a dodecameric, 'double donut,' assembly composed of two face-to-face hexameric rings (Figure 1; [17]). In the presence of Zn^{2+}, Cu^{2+} and other transition metal ions, the dodecamers 'stack' to form protein tubes, and may subsequently associate laterally to yield three- or seven-stranded 'ropes' [18]. The metal-dependent self-assembly process is driven by the formation of intermolecular metal-binding sites at each dodecamer–dodecamer interface. Each dodecamer donates six short amino-terminal α helices that contain His4–X_3–Met8–X_3–His12. The available data suggest that His4 sidechains and His12 sidechains from adjacent dodecamers provide ligands to different metal-binding sites (Figure 1). The resulting protein–protein interface binds 12 metal ions [19–21]. We have explored the utility of *E. coli* GS as a model for rational engineering of protein aggregates with novel self-assembly properties [22,23]. One feature of the GS self-assembly reaction that we have been unable to control previously is the length of tubes generated upon addition of metal ions. The self-assembly process continues until metal ions or protein molecules are exhausted. This limitation is a direct result of the biologically imposed symmetry of the molecule. The methods described here provide a simple basis for alteration of this symmetry, which allows for metal-dependent assembly of dimeric, 'short,' GS tubes that orient with marked axial preference on mica surfaces. In principle, this strategy could be extended to other proteins for which strategically located His tags or cysteines can afford highly oriented protein–resin complexes that result in masking of specific protein surfaces.

Results and discussion

Optimization of on-column modification

We hypothesized that due to multiple, cooperative, binding sites on each flat face of the GS dodecamer, several histidines on the same face of GS would be chelated to a Ni^{2+}-NTA surface. Based on the manufacturer's specifications, a surface density of 0.02 Ni^{2+} atoms/$Å^2$ resin was calculated. Assuming that GS makes a footprint of ~140 × 140 Å on the surface of a bead, then each GS dodecamer would have access to at least ten Ni^{2+} ions, and would have a slow off-rate. Thus, with short times of exposure to the histidine-specific modification reagent diethyl pyrocarbonate (DEPC), only one flat face of the GS structure immobilized on an affinity resin or surface would be modified. This strategy is schematized in Figure 2. Using Figure 1a as a reference, only one blue face

Figure 2

Schematized strategy for asymmetric modification of GS using Ni^{2+}-NTA masking. His4 and His12 residue sidechains on only one face of the GS molecules can chelate the Ni^{2+}-NTA. **(a)** While immobilized, the GS is treated with DEPC (magenta), washed, and eluted with imidazole. **(b)** After removal of imidazole, and addition of metal ions, the asymmetrically modified GS dodecamers self-assemble into dimeric tubes and are growth-arrested.

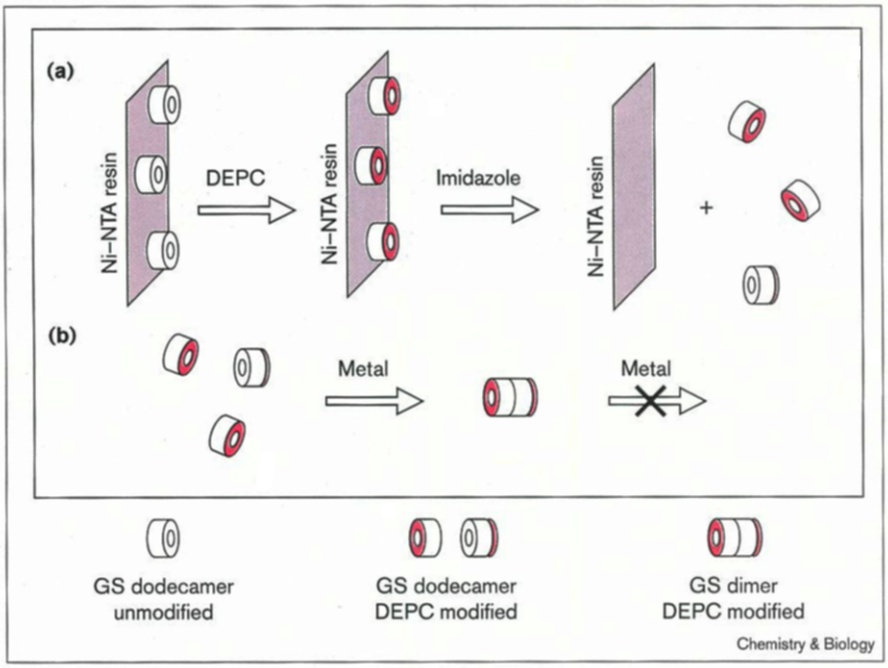

of the GS dodecamer would bind to the Ni^{2+}-NTA resin, and the other face would be exposed. Notably, we showed previously that not all of the His4 or His12 sidechains need to be modified to abolish the stacking behavior [20].

In order to optimize asymmetric modification of GS, several preparations of DEPC-modified GS were obtained by varying the concentration of DEPC chromatographed through the GS-loaded Ni^{2+}-NTA column, and by varying the total time of exposure of immobilized GS to DEPC before washing and eluting. The conditions that afforded the greatest control of the reaction are those described in the Materials and methods section. For five preparations, the extent of modification was 16.5 ± 1.2 His-modified/GS dodecamer. Because of the lability of the DEPC-modified histidine sidechains under conditions required for amino-acid sequence analysis, we were unable to identify the specific residues that were adducted. Presumably, histidine residues other than the His4 and His12 were also modified, but this does not decrease the utility of the strategy. Even with some molecular heterogeneity due to differential labeling, the resulting structures were remarkably homogeneous at the supramolecular level, as shown below.

Characterization of the functional properties of asymmetrically modified GS

In cases where the biological function of protein components used in nanofabrication is important, any strategy used to align or orient proteins must preserve this function. The enzymatic activity of the modified GS was therefore determined and compared with unmodified samples. GS provides an interesting test case because in addition to the histidine residues responsible for tube self-assembly, an active-site histidine (His387) is required for enzymatic activity. Comparison of modification-dependent changes in self-assembly properties and enzymatic activity therefore provides information about the relative specificity of the modification protocol. Here, we have used the standard γ-glutamyl transferase assay to monitor GS activity [20]. Unlabelled GS was used as a standard, to which the activity of modified samples was normalized (100%). GS labeled with DEPC in solution, in the absence of Ni^{2+}-NTA, exhibited 15% of the activity of unmodified GS. In contrast, asymmetrically modified GS retained 55% of the enzymatic activity of the control. As discussed below, the metal-ligating ability of the asymmetrically modified samples was sufficiently altered to yield excellent control over the tube-assembly reaction. Thus, under modification conditions, which yielded increased control over the self-assembly process, significant enzymatic activity was retained. Obviously, the extent to which biological function is altered by asymmetric modification protocols will depend on the modification reagent and the identity of active-site residues.

Characterization of self-assembly properties of asymmetrically modified GS

The self-assembly properties of asymmetrically modified preparations of GS were initially characterized by 90° light scattering (turbidity) and electron microscopy (EM), to determine whether the modification had the expected effect on dodecamer stacking. Whereas unmodified GS

Figure 3

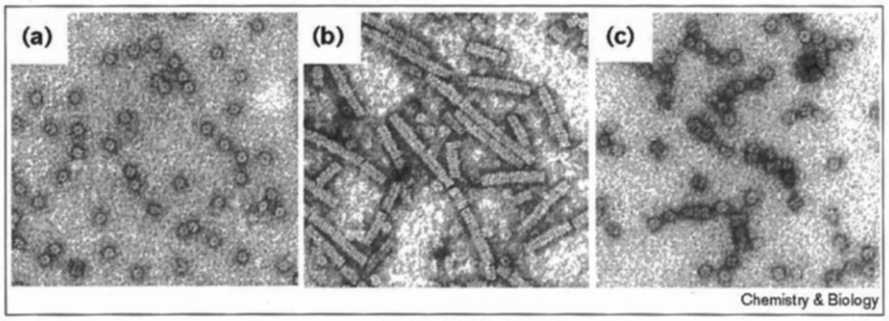

Electron micrographs of asymmetrically modified GS before and after addition of metal ions. **(a)** Asymmetrically modified GS, no Cu^{2+}. Individual dodecamers are observed. **(b)** Unmodified GS + 20 μM Cu^{2+}. Stacked tubes are assembled. **(c)** Asymmetrically modified GS + 20 μM Cu^{2+}. A few dimeric stacks are apparent on their sides, but most molecules are 'face up'.

samples applied to the Ni^{2+}-NTA column and eluted without DEPC treatment readily self-assembled into long tubes after addition of Cu^{2+} or Zn^{2+}, the dodecamers treated on-column with DEPC clearly did not stack to yield long tubes. The turbidity measurements revealed a time- and metal-ion-dependent increase in scattered light intensity much less prominent than observed with tube assembly by unmodified GS, suggesting that either a small fraction of GS molecules were forming tubes, or that the self-assembly process was yielding only aggregates with dramatically reduced dimensions. The EM images revealed only a few dimeric stacks of GS on their sides, after addition of metal ion, however (Figure 3). The orientation of most GS molecules in EM micrographs was face-up, for which it was not possible to distinguish individual GS dodecamers from dimeric stacks. In control experiments, GS modified with DEPC prior to immobilization on Ni^{2+}-NTA did not subsequently bind to the resin or stack in the presence of metal ions, indicating that both of the 'stacking surfaces' were modified.

In order to characterize more rigorously the size distribution of particles present in the, putatively, asymmetrically modified GS, dynamic light scattering (DLS) measurements were performed. DLS provides a sensitive probe of the aggregation state directly in solution, without additional manipulation or staining [24]. The distributions of particle sizes present in solution are summarized in Figure 4, for various samples. For the GS-modified with DEPC on the Ni^{2+}-NTA resin, addition of metal ion caused a 1.9 ± 0.2-fold increase in the mean particle size. Also shown, are results for the addition of Cu^{2+} to unmodified GS, which yields a broad distribution of tubes ranging from 6–12-fold larger in apparent size than the

Figure 4

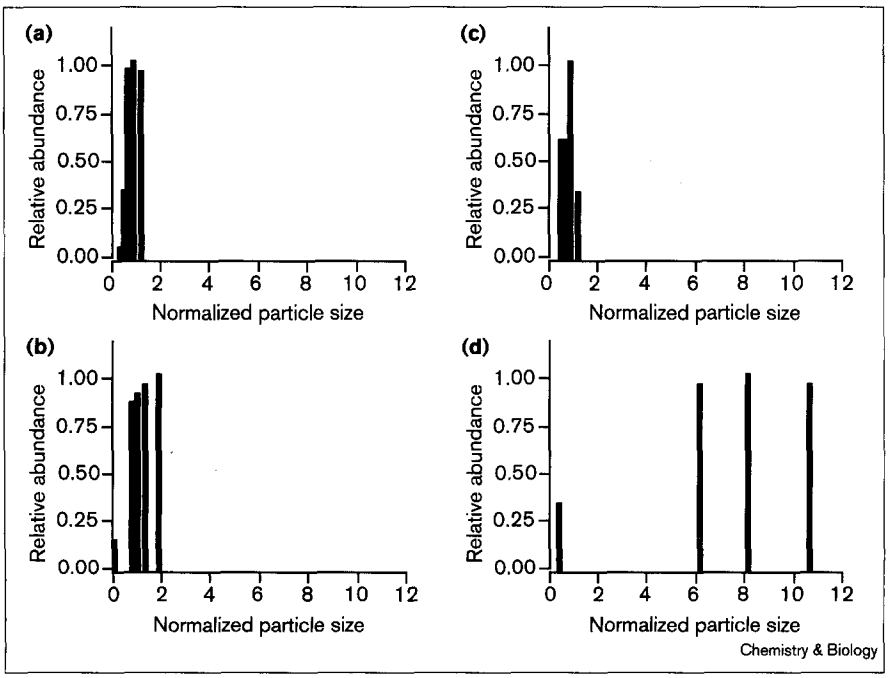

Dynamic light scattering. **(a)** Asymmetrically modified GS, no Cu^{2+}. **(b)** Asymmetrically modified GS + 20 μM Cu^{2+}. The mean particle size increases twofold compared to (a). **(c)** Unmodified GS, no Cu^{2+}. **(d)** Unmodified GS + 20 μM Cu^{2+}. A wide distribution of particles sizes is obtained that are 6–12-fold larger than GS dodecamers. Particle sizes are normalized to GS dodecamers in the absence of metal ions. Because no shape analysis has been performed, sizes are 'apparent.'

Figure 5

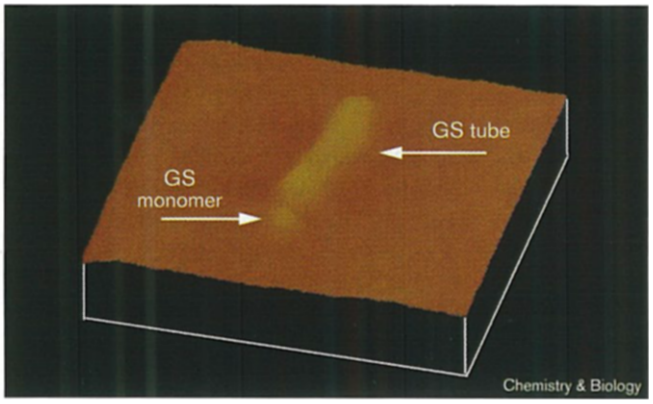

Atomic force microscopy image of GS. A GS monomer oriented face-up lies at the end of a self-assembled tube. The inverted 'i' demonstrates the facile distinction between particles observed, including the difference in vertical heights for GS dodecamers oriented face-up (GS monomer) versus edge-on (GS tube).

unstacked GS dodecamers. When Cu^{2+} was added to GS dodecamers treated with DEPC in solution, in the absence of Ni^{2+}-NTA resin, there was no shift in the particle size, which remained centered at a size corresponding to individual GS dodecamers (data not shown). The DLS results indicated that the asymmetrically modified samples do not form large tubes, as indicated also by EM, but they do aggregate in the presence of metal ions. Moreover, the size of the aggregates based on DLS is consistent with the formation of growth-arrested dimeric stacks, as suggested by the scheme in Figure 2. From these results, it remained unclear whether the particles observed by EM were dimeric stacks oriented face-up, or individual GS dodecamers resulting from a staining and mounting procedure that disrupted the aggregate structure that had formed in solution.

An independent method for determining the aggregation state and surface orientation of particles was therefore sought using tapping-mode atomic force microscopy (AFM). AFM provides direct measurement of dimensions for particles on a surface, including 'height' above the surface [25]. For biological molecules, absolute dimensions measured by AFM may be inaccurate due to lateral expansion or vertical compression. Many proteins, however, have been visualized using AFM and, when appropriate standards are available, precise relative dimensions can be obtained. The GS system is particularly suited to this analysis because the available X-ray structures [17] provide a reference for relative dimensions along each molecular axis. For example, in X-ray structures the outer diameter of the GS ring is 140 Å, whereas the axial length of the dodecamer is 107 Å, resulting in an axial ratio of 1.30. This ratio of vertical heights would be expected also for AFM images, if measured for a dodecamer sitting on-edge versus face-up. The vertical dimensions for GS dodecamers sitting face-up versus edge-on is apparent in the three-dimensional AFM image in Figure 5, which reveals a GS dodecamer face-up near the end of a self-assembled tube. The resulting 'i' structure contains all of the necessary vertical and lateral dimensions required to characterize GS particles of different aggregation states. When GS molecules clearly lie on-edge, as in self-assembled tubes, then the vertical height provides a benchmark for the outer diameter of the ring (Figure 6b). For these structures, the lateral dimension across the tube provides a benchmark for the same molecular dimension along a horizontal axis. Section analyses of AFM images of the asymmetrically modified GS before and after addition of metal are also shown in Figure 6. In the absence of Cu^{2+} (Figure 6a), individual GS dodecamers that have been asymmetrically modified afford vertical and lateral dimensions of 73 Å and 96 Å, corresponding to a face-up orientation with an axial ratio of 1.32, in excellent agreement with the ratio

Figure 6

Atomic force microscopy of GS and various aggregation states. Images are shown for the section analyses, two-dimensional perspective, on top. **(a)** A single GS dodecamer. **(b)** A GS tube obtained from unmodified GS in the presence of Cu^{2+}. **(c)** A GS modified with DEPC while bound to Ni^{2+}-NTA, in the presence of Cu^{2+}. The vertical dimension in (c) is 2.02-fold larger than the monomer and 1.63-fold larger than the outer diameter of the GS ring.

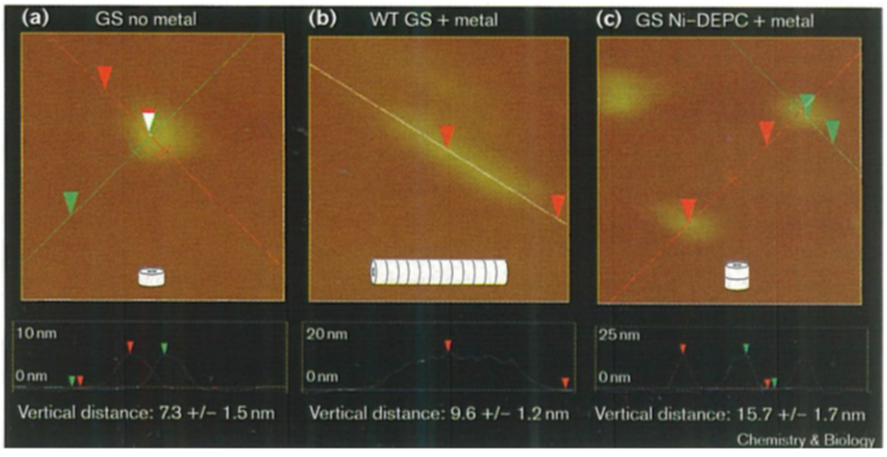

Figure 7

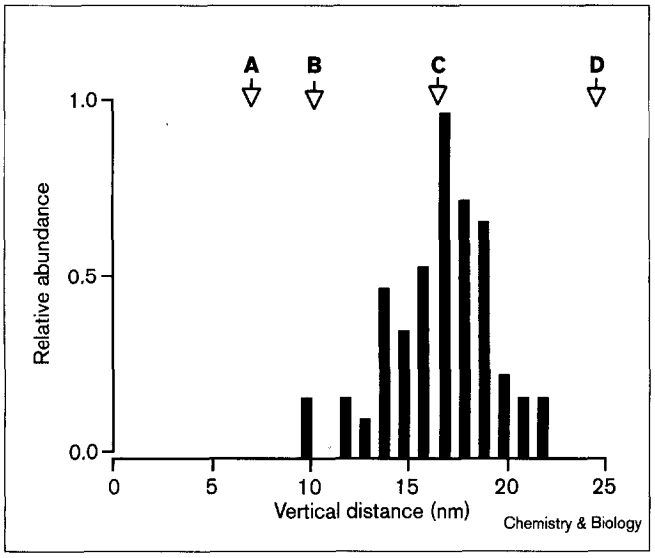

Distribution of particle sizes determined using AFM. Several AFM fields of asymmetrically modified GS were subjected to detailed analysis. The vertical heights (n = 68, four fields) were determined, and the relative abundance is plotted. Vertical heights are indicated by arrows for: A, face-up GS monomer; B, edge-on monomer; C, face-up dimer; D, face-up trimer. The homogeneous distribution is centered at the height expected for face-up dimers.

predicted by the X-ray structure. In the presence of Cu^{2+} (Figure 6c) the vertical height increases 2.02-fold compared with metal-free samples and the axial ratio is completely consistent with dimeric stacks oriented with the sixfold axis of symmetry normal to the surface. Furthermore, the ratio of vertical heights of the dimeric stacks to the ring outer diameter is 15.7/9.9 = 1.63, in agreement with the ratio predicted by the X-ray structure, 1.53. Interestingly, the population of dimeric GS stacks is nearly uniform in its orientation, based on analyses of several fields and preparations, which indicate a monodisperse population on the surface. In fact, detailed analysis of several particles in different AFM fields reveals a remarkable degree of homogeneity in the particle size for asymmetrically modified samples. The distribution of vertical heights measured for 68 individual particles from four fields is summarized in Figure 7. The population is centered at a particle size corresponding to face-up dimers. Essentially no free monomers or face-up trimers are observed, although a small fraction of molecules on edge (monomers or dimers) may be indicated by the presence of a few particles with vertical height 10 Å. The marked preference for face-up orientation on the mica surface was fortuitous, but the AFM results further support the suggestion that the EM images correspond to dimeric GS stacks sitting face up. The combination of EM, DLS and AFM indicate the success of the strategy outlined in Figure 2.

Extension to other functional groups and use of asymmetrically modified GS as a 'molecular cap'

The utility of Ni^{2+}-NTA as a chemical mask would be extended greatly if amino-acid sidechains other than histidine could be incorporated into the strategy. In order to explore this possibility, we attempted to asymmetrically modify a variant of GS, Met8→Cys (M8C), which contains a surface cysteine between each His4 and each His12 residue (Figure 1). We hypothesized that cysteine-specific modification reagents would be inaccessible to Cys8 residues on the GS surface immobilized on Ni^{2+}-NTA due to steric constraints. By analogy, the asymmetrically modified M8C would be rendered incapable of metal-dependent stacking on one face, due to steric constraints. For these experiments, we exploited the cysteine-specific fluorescent probe 7-diethyl-3-(4′-maleimidylphenyl)-4-methylcoumarin (CPM), and performed on-resin modification to obtain 4.3 ± 1.0 CPM/dodecamer. The wild-type GS was not labeled with CPM under identical conditions, due to the lack of surface exposed cysteine residues. M8C samples labeled with CPM according to the scheme in Figure 2 exhibited similar metal-dependent self-assembly properties as the asymmetrically DEPC-modified GS (data not shown). Specifically, the M8C preparations formed dimeric stacks in the presence of Cu^{2+} or Zn^{2+}. We hypothesized further that the asymmetrically modified GS could be used as a 'molecular cap,' and stack at the end of a growing GS tube to prevent further addition of GS dodecamers. We have shown previously that unmodified M8C stacks at least as efficiently as wild-type GS [19]. Thus, if varying ratios of unmodified M8C and asymmetrically modified M8C–CPM were mixed with metal ions, tubes of intermediate length would dominate the final population. Progress curves for stacking of reaction mixtures containing variable ratios of unmodified and asymmetrically modified M8C–CPM are shown in Figure 8a, where the total protein concentration increases, and the concentration of unmodified M8C is held constant. The growth arrest of tubes is, therefore, not due to exhaustion of protein components. As expected, the mean tube length varied with ratio of protein components, although heterogeneity at each ratio is still apparent by EM (Figure 8b–d). In effect, the asymmetrically modified M8C–CPM dodecamers are inhibitors of the self-assembly process when unmodified M8C dodecamers are present. A point of central importance is that such inhibitors are inaccessible by recombinant DNA methods alone. Although the data set is limited, it appears that the apparent 'K_i' for inhibition of GS self-assembly by asymmetrically modified M8C–CPM is ~50 nm. These results not only confirm the success and utility of the asymmetric modification described above, but they also suggest the potential utility of the strategy for modification of residues other than histidine to expand the range of components available for protein-based devices.

Figure 8

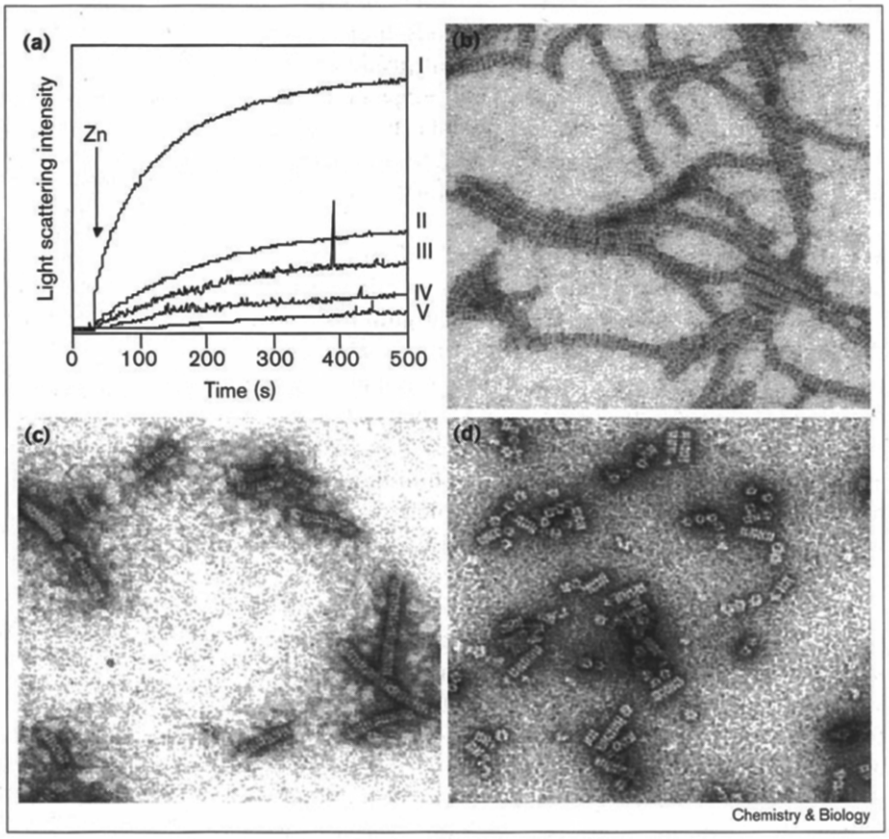

Asymmetrically modified GS as a molecular cap. **(a)** Progress curves for M8C stacking after addition of Zn^{2+} at variable ratios of asymmetrically modified M8C–CPM GS:unmodified M8C. The CPM-labeled M8C inhibits the stacking reaction. All samples contained 50 μg protein/ml unmodified M8C. I, no asymmetrically modified GS. II, III, IV, V contained 0.2:1, 0.6:1, 0.8:1, 1:1 modified M8C–CPM:unmodified M8C. **(b)** EM micrograph of I. **(c)** EM micrograph of III. **(d)** EM micrograph of V.

Specific applications of the asymmetric modification protocol, as applied to other proteins, can be envisioned by analogy to other engineered proteins with distinct recognition surfaces. For example, drug-delivery protocols have been suggested that exploit biotin–streptavidin interactions [16]. Denatured streptavidin variants *in vitro* may afford asymmetric chimeras upon refolding, with distinct biotin-binding sites on 'opposite' faces of the tetramer. In proposed drug-delivery schemes, one face of the asymmetric streptavidin tetramer is loaded at the 'high-affinity' biotin-binding sites with a biotinylated tumor-specific antibody. The biotinylated antibody then delivers the streptavidin to the tumor. Subsequent dosing with biotinylated antitumor drug results in localization of the drug near the tumor, via the 'low-affinity' binding sites remaining on streptavidin. A critical step in such 'pre-targeting' drug-delivery protocols is the ability to generate chimeric, asymmetric proteins with distinct binding sites on previously equivalent subunits. Indeed, it would be interesting to explore our on-column modification strategy to 'load' biotin-binding sites on one-face of the streptavidin tetramer, through engineered interactions with Ni^{2+}-NTA.

An additional example of the utility of asymmetric modification may be found in chromatographic 'adapters.' Fusion proteins are commonly used to introduce desired chromatographic properties into a protein of interest [8,9,26]. In principle, proteins such as GS could be used to immobilize other proteins, for example on Ni^{2+}-NTA, by asymmetrically modifying a surface cysteine (such as the Met8→Cys GS mutant with a suitable affinity ligand. Proteins with affinity for this ligand, but which contain surface-accessible histidine, would be expected to be retained on the resin and easily eluted with free ligand. In analogous applications, 'adapters' molecules have been used to sequentially layer proteins on surfaces in the fabrication of biosensors and biomaterials. In these cases, adapters are used to achieve desired surface orientation of discrete layers of proteins or ligands. Here, the GS could act as an 'adapter' for immobilization of proteins unsuitable for incorporation of a His-tag, via cysteine-linked affinity reagents. Notably, the exceptional stability of GS [27], the availability of large quantities through bacterial expression systems, as well as the simple purification of wild-type and variant GSs add to the potential utility of asymmetrically modified GS.

Significance

Fabrication of novel protein-based materials requires control of spatial and topological arrangement of the

individual components in complex aggregates, either in solution or on surfaces. Often, such control can be achieved by recombinant DNA methods that incorporate molecular recognition 'handles' at predetermined sites within the folded protein. The range of proteins available for molecular devices would be expanded, however, if biologically imposed symmetry of oligomeric proteins could be controlled by *in vitro* methods.

We have characterized the utility of an affinity 'surface' as a chemical mask in order to eliminate the symmetry of the biologically assembled glutamine synthetase (GS), and to gain control of a self-assembly process, by selective protection of a subset of histidine or cysteine residues on its surface. An attractive feature of this strategy is its simplicity. In addition, it is possible to envision a modular approach combining genetic methods and chemical masking in which two or more modification reagents can be incorporated, in order to fabricate complex arrays of chemical moieties. For example, engineered cysteines and histidines could be expressed on all equivalent surfaces of any symmetrical protein, and subsequently modified asymmetrically *in vitro* on the same face or on opposite faces, by adapting the scheme in Figure 2 accordingly. Moreover, the modification reagents are not limited to small organic molecules. Peptides and proteins could be attached selectively on a single face of an immobilized protein molecule that presents cysteines for disulfide-bond formation, and enzymatic modification by proteases, for example, could be limited to one face. The facile incorporation of histidine at any desired location within folded protein structures, suggests the general applicability of Ni^{2+}-NTA as a mask to control chemical modification of many amino-acid functional groups with a wide range of reagents. The results described here provide 'proof of principle' that biologically imposed symmetry can be controlled using *in vitro* methods.

The results described here also demonstrate the potential utility of the protocol for fundamental research. The complexity of the GS system, including the tendency of self-assembled tubes to aggregate laterally, has hampered quantitative analysis of the forces responsible for interaction at individual dodecamer–dodecamer interfaces. Even fundamental parameters describing this interaction, such as the dissociation binding constant (K_d), have been elusive. As a result of gaining control of the self-assembly reaction, it should be possible to determine thermodynamic and kinetic parameters for metal-dependent GS docking that have been experimentally inaccessible for the unmodified GS. The study of other proteins that form complex aggregates with multiple interacting surfaces could also be 'simplified' by similar procedures, therefore enhancing the accessibility of fundamental parameters.

Materials and methods

Protein purification and expression

The construction, expression and purification of the proteins used here have been described previously [19,20].

Protein modification with DEPC

Wild-type or mutant GS (5 mg) was loaded on a 2 ml Ni^{2+}-NTA column (Qiagen®) equilibrated with 50 mM Hepes, pH 7.2, 100 mM KCl, 1.0 mM $MnCl_2$ (equilibration buffer), at 25°C. After washing with five column volumes of equilibration buffer, the resin was exposed to five column volumes of equilibration buffer containing 0.5 mM DEPC (Sigma, St. Louis, MO), at a flow rate of ~0.5 ml/min. The column was washed with an additional five column volumes of equilibration buffer lacking DEPC. Approximately 5% of the loaded protein was eluted in this wash. The remaining protein was eluted with 10 ml of 20 mM imidazole. Fractions containing protein were pooled, concentrated and chromatographed over Sephadex G25 in equilibration buffer. Extent of modification was determined by the method of Miles [28], using the absorbance at 230 nm, 240 nm and at 280 nm, and known extinction coefficients for ethyl carbonate-modified histidine of $\varepsilon_{240} = 3200\ cm^{-1}\ M^{-1}$ and $\varepsilon_{230} = 3000\ cm^{-1}\ M^{-1}$, respectively. In order to obtain reproducible results, it was essential that DEPC was freshly diluted from a dry (Nitrogen purged) stock for each experiment.

Protein modification with CPM

Modification with CPM (Molecular Probes, Eugene OR) was identical to the conditions described for DEPC modification, except that 10 column volumes of equlibration buffer containing 100 μM CPM were used for the modification. In addition, it was observed that CPM was hydrolyzed from the protein upon long-term storage. Therefore, all experiments were performed within 24 h of labeling. Extent of modification was determined from $\varepsilon_{385} = 32{,}000\ cm^{-1}\ M^{-1}$, as provided by the manufacturer.

Electron microscopy and turbidity measurements

All EM and turbidity measurements were as described previously [19–22].

Dynamic light scattering

All reagents used for DLS were filtered through a 0.22 μM filter, prewashed with 0.1 N HCl. Samples initially at 50 μg protein/ml in equilibration buffer with or without 10 μM Cu^{2+} were diluted 25-fold into the same buffer, to a final volume of 10 ml. The presence of metal ion in the absence of protein had no effect on 'baseline' scattering. Particle size was determined with a Brookhaven saphire laser spectrometer (Brookhaven Inst, NY) by analyzing the scattering fluctuations detected at a 45° scattering angle. The autocorrelation function was averaged over 10 μs with a Brookhaven 9000AT autocorrelator, using the CONTIN method [29].

Atomic force microscopy

Samples eluted from the Ni^{2+}-NTA resin, containing 50 μg protein/ml in 50 mM Hepes, pH 7.4, 100 mM KCl and 1 mM $MnCl_2$, were made 10 μM Cu^{2+}. Samples were diluted to 100 ng protein/ml, maintaining 10 μM Cu^{2+}. Solution was placed on freshly cleaved mica for 30 min, and the surface was rinsed with distilled H_2O. Samples were dried under a stream of N_2. Tapping-mode AFM was performed with a Nanoscope III AFM (Digital Instruments, Santa Barbara, CA) operating in air. Etched silicon cantilevers oscillating at 250–270 kHZ were used. Nominal tip radius was 5–10 nm. Images were obtained in the height mode and analyzed with section analyses.

Acknowledgements

The authors gratefully acknowledge Eric Dietze and Claudia Jochheim for helpful discussion, and The University of Washington Center for Nanotechnology for use of instrumentation. This work was supported by The Petroleum Research Fund (PRF 31565, WMA) and The National Science Foundation (MCB9305202, W.M.A. and OPP9615197, W-C.C.)

References

1. Laval, J.M., Chopineau, J. & Thomas, D. (1995). Nanotechnology: R & D challenges and opportunities for application in biotechnology. *Trends Biotechnol.* **13**, 474-481.
2. Wilner, I. & Wilner, B. (1997). Photo-switchable biomaterials as ground for optobioelectronic devices. *Bioelec. Bioenerg.* **42**, 43-57.
3. Voyer, R. (1997). The development of peptide nanostructures. *Bioorg. Chem.* **184**, 1-37.
4. Mrksich, M., Grunwell, J.R., & Whitesides, G.M. (1995). Biospecific adsorption of carbonic anhydrase to self-assembled monolayers of alkanethiolates that present benzenesulfonamide groups on gold. *J. Am. Chem. Soc.* **117**, 12009-12010.
5. Blawas, A.S. & Reichert, W.M. (1998). Protein patterning. *Biomaterials* **19**, 595-609.
6. Hartgerink, J.D., Granja, J.R., Milligan, R.A. & Ghadiri, R. (1996). Self-assembling peptide nanotubes. *J. Am. Chem. Soc.* **118**, 43-50.
7. Boncheva, M. & Vogel, H. (1997). Formation of stable polypeptide monolayers at interfaces: controlling molecular conformation and orientation. *Biophys. J.* **73**, 1056-1072.
8. Damrongchai, N., Yun, K., Kobatake, E. & Aizawa, M. (1997). Self-assembling of glutathione S-transferase/calmodulin fusion protein on chemically modified gold surface. *J. Biotechnol.* **55**, 125-133.
9. Stahl, S., Lundeberg, J., Uhlen, M. & Nygren, P.A. (1997). Affinity fusion strategies for detection, purification and immobilization of recombinant proteins. *Prot. Express. Purif.* **11**, 1-16.
10. Stayton, P.S., Olinger, J.M., Jiang, M., Bohn, P.W. & Sligar, S.G. (1992). Genetic engineering of surface attachment sites yields oriented protein monolayers. *J. Am. Chem. Soc.* **114**, 9298-9299.
11. Dietrich, C., Schmitt, L. & Tampe, R. (1995). Molecular organization of histidine-tagged biomolecules at self-assembled lipid interfaces using a novel class of chelator lipids. *Proc. Natl Acad. Sci. USA* **92**, 9014-9018.
12. Frey, W., *et. al.*, & Arnold, F.H. (1996). Two-dimensional protein crystallization via metal-ion coordination by naturally occurring surface histidines. *Proc. Natl Acad. Sci. USA* **93**, 4937-4941.
13. Suh, S-S., Haymore, B.L. & Arnold, F.H. (1991). Characterization of His-X_3-His sites in α-helices of synthetic metal-binding bovine somatotropin. *Prot. Eng.* **4**, 301-305.
14. Schmid, E.L., Keller, T.A., Dienes, Z. & Vogel, H. (1997). Reversible oriented surface immobilization of functional proteins on oxide surfaces. *Anal. Chem.* **69**, 1979-1985.
15. Dontha, N., Nowall, W.B. & Kuhr, W.G. (1997). Generation of biotin/avidin/enzyme nanostructures with maskless photolithography. *Anal. Chem.* **69**, 2619-2625.
16. Chilkoti, A., Schwartz, B.L., Smith, R.D., Long, C.J. & Stayton, P.S. (1995). Engineered chimeric streptavidin tetramers as novel tools for bioseparations and drug delivery. *Biotechnology* **13**, 1198-1204.
17. Almassy, R.J., Janson, C.A., Hamlin, R., Xuong, N.H. & Eisenberg, D. (1986). Novel subunit interactions in the structure of glutamine synthetase. *Nature.* **323**, 304-309.
18. Frey, T.G., Eisenberg, D. & Eiserling, F.A. (1975). Glutamine synthetase forms three- and seven-stranded cables. *Proc. Natl Acad. Sci. USA* **72**, 3402-3406.
19. Dabrowski, M.J., Yanchunas, J. Jr., Villafranca, B.C., Dietze, E.C., Schurke, P.J. & Atkins, W.M. (1994). Supramolecular self-assembly of glutamine synthetase: mutagenesis of a novel intermolecular metal binding site required for dodecamer stacking. *Biochemistry* **33**, 14957-14964.
20. Yanchunas, J., Dabrowski, M.J., Schurke, P.J. & Atkins, W.M. (1994). Supramolecular self-assembly of *E. coli* glutamine synthetase: characterization of dodecamer stacking and high-order association. *Biochemistry* **33**, 14949-14956.
21. Atkins, W.M. (1994). Supramolecular self-assembly of *E. coli* glutamine synthetase: effects of pressure and adenylylation state on dodecamer stacking. *Biochemistry* **33**, 14965-14973.
22. Dabrowski, M.J., Chen, J.P. & Atkins, W.M. (1997). Synthesis and characterization of supramolecular protein aggregates: self-assembled, molecularly-ordered, protein tubes from electrostatic complementation of glutamine synthetase dodecamers. *Protein Eng.* **10**, 1289-1294.
23. Dabrowski, M.D. & Atkins, W.M. (1995). Engineering macromolecular self-assembly: molecular tubes vs. protein sheets via single amino acid substitutions in *E. coli* glutamine synthetase. *Adv. Mater.* **7**, 1015-1017.
24. Janmey, P.A. (1993). Application of dynamic light scattering to biological systems. In *Dynamic Light Scattering: The Method and Some Applications* (Brown, W., ed.), University Press, New York. **5**, 611-651.
25. Hansma, H.G. & Hoh, J. (1994). Biomolecular imaging with the atomic force microscope. *Ann. Rev. Biophys. Biomol. Struct.* **23**, 115-139.
26. Hentz, N.G. & Daunert, S. (1996). Bifunctional fusion proteins of calmodulin and protein A as affinity ligands in protein purification and in the study of protein-protein interactions. *Anal. Chem.* **68**, 3937-3944.
27. Shrake, A., Fisher, M.T., McFarland, P.J. & Ginsburg, A. (1989) Partial unfolding of dodecameric glutamine synthetase from *Escherichia coli*: temperature-induced reversible transitions of two domains. *Biochemistry* **28**, 6281-6294.
28. Miles, E.W. (1977). Modification of histidyl residues in proteins by diethyl pyrocarbonate. *Methods Enzymol.* **47**, 431-442.
29. Provencher, S.W.A. (1982). Constrained regularization method for inverting data represented by linear algebraic or integral equations. *Comput. Phys. Commun.* **27**, 213-227.

Because *Chemistry & Biology* operates a 'Continuous Publication System' for Research Papers, this paper has been published via the internet before being printed. The paper can be accessed from http://biomednet.com/cbiology/cmb – for further information, see the explanation on the contents pages.